A. M. Essling, *Phys. Rev. C* 22, 750 (1980)].
50. We thank the other members of the New Guinea field expedition of 1988, particularly E. Wallensky who facilitated all aspects of the field research; M. Stuiver, E. A. Boyle, S. J. Lehman, D. Lea, K. Kelts, H. E. Wright, Jr., T. Brazuinas, B. Haskell, M. Abbott, C. D. Gallup, D. A. Richards, and two anonymous reviewers for helpful comments and discussions; and J.W.B. for important contributions to the interpretation of our data. Supported by National Science Foundation (NSF) grants EAR-8804970 (A.L.B.), EAR-8904705 (R.L.E.), ATM-8904987 (F.W.T.), OCE-8915919 (E.R.M.D.), and ATM-8921760 (R.L.E.); and, for the TIMS analytical facility, by NSF grant EAR-8817260 (R.L.E.) and the University of Minnesota.

22 December 1992; accepted 19 April 1993

Beach Cusps as Self-Organized Patterns

B. T. Werner and T. M. Fink

Computer simulations of flow and sediment transport in the swash zone on a beach demonstrate that a model that couples local flow acceleration and alongshore surface gradient is sufficient to produce uniformly spaced beach cusps. The characteristics of the simulated cusps and the conditions under which they form are in reasonable agreement with observations of natural cusps. The self-organization mechanism in the model is incompatible with an accepted model in which standing alongshore waves drive the regular pattern of erosion and deposition that gives rise to beach cusps. Because the models make similar predictions, it is concluded that currently available observational data are insufficient for discrimination between them.

Beach cusps are uniformly spaced, arcuate scallops in sediment that form at the shoreward edge of the episodically exposed portion of a beach known as the swash zone. Beach cusps and other regular topographic features in the nearshore, including ripples, megaripples, sand bars, ridges and runnels, sand waves, and swash marks (*1*), have attracted investigation owing to their beauty, their effect on sediment transport, and their uniformity in the presence of complex interactions between waves, currents, and sediment. According to a widely accepted hypothesis, the form and spacing of beach cusps reflect a pattern of alongshore standing waves on the beach (*2–4*). An alternative, physically incompatible model ascribes cusp formation to feedback between swash flow and beach morphology. This model has been discounted partially because of the difficulty of understanding how local interactions between fluid and sediment lead to globally uniform patterns (*4*). Using computer simulations, we show that uniform beach cusps can develop by local flow-morphology feedback, examine the implications of this self-organization model, and demonstrate that the predictions of the standing wave and self-organization models are sufficiently similar that current data and observations cannot distinguish unambiguously between them.

Beach cusps form on oceanic and lacustrine beaches and in sediments ranging from fine sand to cobbles. They result from a varying combination of accretion at cusp horns and erosion in the interjacent cusp bays (*1*). Cusps are typically spaced 10 cm to 60 m apart (*1*). Beach cusp formation is favored under conditions of surging, nonbreaking waves of near-normal incidence on steep (usually coarse-grained) beaches (*1, 5*). Swash runs up a beach without cusps as a thinning, often irregular sheet. On a cuspate beach, runup is deflected by horns toward bays and from there flows seaward as runout.

In the self-organization model, incipient topographic depressions in a beach are amplified by attracting and accelerating water flow, thereby enhancing erosion (Fig. 1A) (*5*). Dean and Maurmeyer (6) related well-developed beach cusp spacing to the swash excursion, the horizontal distance between the highest and lowest positions of the swash front on a beach, by considering the kinematical trajectory of elastic particles sliding on the surface of a cusp.

In contrast, according to the standing-wave model, the pattern of erosion and deposition of sediment leading to beach cusps originates with the flow patterns of alongshore standing waves (*2–4, 7, 8*), generally taken to be subharmonic edge waves (Fig. 1B), which are trapped waves with half the frequency of incident waves. The standing wave model successfully predicts beach cusp spacing as a function of incident wave frequency and beach slope within about a factor of 2 (*4, 9*) (compatible with uncertainties in model input parameters). In addition, standing waves induce cusp formation in sand at the swash zone margin on a laboratory concrete beach (*3*). However, because subharmonic edge waves decay strongly within one incident wavelength of the shore, they are difficult to detect. Standing subharmonic edge waves have not been observed unambiguously in conjunction with beach cusp formation in the field (*10*).

Our simulation algorithm uses a simplified model of coupled flow, sediment transport, and morphology change with the goal of simulating the evolution of cusps from arbitrary initial morphology. In contrast, earlier models considered wave and fluid flow interactions with a plane (*3, 7*) or a regular cuspate beach (*6, 8*) only. We are able to investigate the development of uniform cusps, rather than postulating their uniformity and general form, and to simulate explicitly conditions under which cusps do not form.

Our model treats only the kinematics in gravity of swash flow over a beach (*6*), without directly considering the hydrodynamics of swash. This approximation is supported by an inviscid calculation (*11*) and laboratory measurements (*12*) on the motion of the swash front (the leading edge of the swash). Flow is simulated by cubical water particles, representing the swash front, that move according to Newton's laws in gravity (the kinematical equations) and are constrained to remain on the surface of the beach. For example, water particles move on parabolas in the swash zone on a plane beach (Fig. 2A). In addition to the gravitational force, water particles are repelled from regions of high water particle concentration and are attracted toward regions of low concentration in a simplified approximation to flow caused by pressure gradients induced by the sea surface.

The simulated beach is composed of thin, square slabs of sediment stacked on a rectangular grid of square cells with periodic

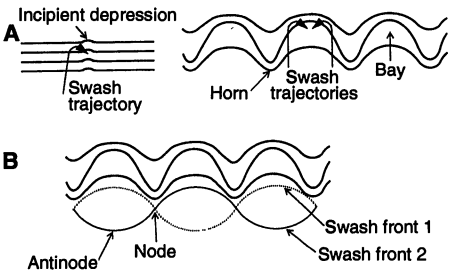

Fig. 1. Self-organization and standing wave models. Seaward is down. Bold lines are beach contours. (**A**) (Left) Deflection of swash flow by incipient topographic depression causing further erosion; (right) swash zone circulation in equilibrium with beach cusps (*6*). (**B**) Alignment of beach cusps and sinusoidal variation in the swash front caused by subharmonic edge waves shown at two consecutive swash cycles as broken and solid lines (*3*). Nodes in the swash excursion align with cusp horns.

B. T. Werner, Center for Coastal Studies, Scripps Institution of Oceanography, La Jolla, CA 92093–0209.
T. M. Fink, Division of Physics, Mathematics and Astronomy 200-36, California Institute of Technology, Pasadena, CA 91125.

boundary conditions in the alongshore direction. The water particles erode, transport, and deposit sediment slabs according to a sediment carrying capacity that varies as the square of the water particle velocity. Thus, sediment flux is proportional to the cube of flow velocity, in agreement with many bedload transport theories (*13*). Water particles deposit sediment slabs in the cell they occupy when decelerating and erode sediment when accelerating. If deposition of a sediment slab increases the local beach slope beyond a maximum angle of repose, the slab is moved down the steepest gradient until no surface angle exceeds the angle of repose. So that erosion and deposition are distributed beyond the cells that contain water particles, the elevation of a cell occupied by a water particle and the elevations of the surrounding region are smoothed by rearranging the sediment slabs to minimize local variation from a plane. Velocity-dependent erosion and deposition tend to increase relief, whereas smoothing and enforcement of the angle of repose decrease slopes and communicate elevation changes among nearby cells.

The simulation begins with an alongshore line of water particles at the seaward edge of a plane beach (Fig. 2A). The water particles initially are given a nearly uniform shoreward velocity ($= \sqrt{2g\tan\beta S}$, where g is the acceleration of gravity, $\tan\beta$ is the beach slope, and S is the cross-shore swash excursion) that remains constant until the particles reach a specified beach elevation that demarcates the seaward edge of the swash zone. For a smooth transition to the swash zone, the sediment carrying capacity varies linearly with elevation to a maximum value at the bottom of the swash zone. In the swash zone, water particle motion and sediment transport are as described above. After moving seaward of the swash zone, water particles again travel at constant velocity and their carrying capacity is proportional to elevation. Each iteration of this procedure represents a swash cycle. Deficiencies in this approach include the assumption that flow and sediment transport in the swash zone can be described adequately by motion at the swash front and that the interaction between the runout of one swash cycle and the runup of the next can be ignored (*6*).

The development of uniformly spaced simulated beach cusps from a plane beach requires 50 to 1000 swash cycles (corresponding to roughly 0.1 to 3 hours for 10-s waves), depending on cusp spacing and the parameters chosen (Fig. 2). Cusp formation is robust to changes in parameters and alterations to the specific form of the algorithm; for example, elimination of water particle interactions, changes to the sediment transport law, the introduction of energy dissipation, or the use of an algorithm in which water particles move straight up the beach and follow the steepest gradient down the beach all result in cuspate forms with a regular spacing that varies by less than a factor of 3. Deltas form offshore of cusp bays, and depressions form offshore of cusp horns (Fig. 2B), as observed on natural cusps (*5*).

Simulated beach cusps develop through a combination of (i) positive feedback between morphology and flow that creates incipient relief and (ii) negative feedback that inhibits net deposition or erosion on well-formed cusps. Random alongshore topographic depressions form in the initially plane beach as a result of slightly different initial water particle trajectories or the random order in which the algorithm moves water particles and deposits or erodes sediment. Depressions cause acceleration of the water particles, resulting in enhanced erosion and an increase in relief. For example, on a beach with a 5° slope, depressions with local slope variations more than 0.5° increase in depth. Erosion of topographic lows occurs preferentially on the runout. Similarly, swash particles that move over topographic highs decelerate and deposit sediment, preferentially on the runup. Topographic lows can evolve to cusp bays, and topographic highs to cusp horns. Communication of surface gradients by smoothing and by interactions between water particles facilitates the establishment of regular cusps. This spontaneous development of a global cusp pattern through local interactions is characteristic of self-organization.

On simulated cusps, the swash circulation pattern resembles that on natural cusps; water particles are deflected by cusp horns to collide in the center of cusp bays and, from there, move seaward (Fig. 2C). This circulation pattern results in no net

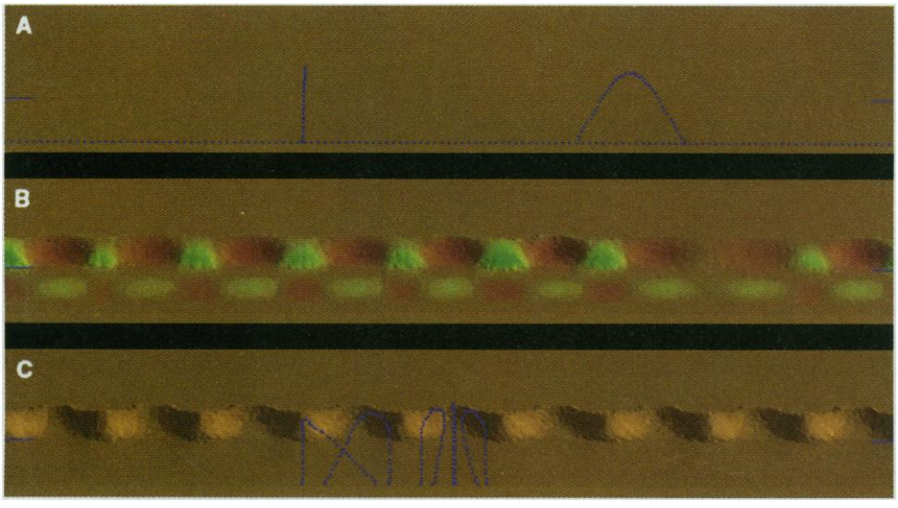

Fig. 2. Simulated beach cusp development from a plane beach in a 400 cell by 180 cell simulation. Seaward is down. Bottoms of swash zones are marked by blue lines on both sides. Sediment slab dimensions, 0.1 m by 0.1 m by 0.0005 m; beach slope, 10°; S = 1.8 m; and f = 2.5. On a plane beach, each water particle deposits a layer of sediment 6 mm thick on runup and erodes a 6-mm layer on runout. On average, a five cell by five cell area surrounding a water particle is smoothed each time it moves over a new cell. (**A**) Initial plane beach with water particles at bottom in blue. Water particle trajectories shown are linear seaward of the swash zone and parabolic in the swash zone. (**B**) Initial development of morphology after 100 swash cycles. Regions of erosion (from the initial plane beach) are shown in red and regions of deposition are in green. Note deposition offshore of cusp bays and erosion offshore of cusp horns. (**C**) Uniformly spaced beach cusps after 250 swash cycles. Trajectories of water particles deflected from horns to bays are shown in blue.

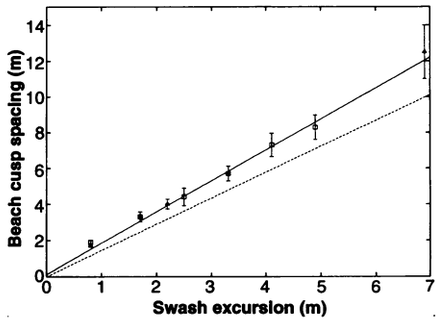

Fig. 3. Measured mean beach cusp spacing versus measured swash excursion for simulated cusps. Swash excursion was changed by varying the beach slope (triangles) and initial runup velocity (squares). Simulated beach cusp spacing varies linearly with swash excursion. Solid line shows best fit with slope f = 1.7, in agreement with one value, 1.6, obtained from natural cusps (*6*). Dashed line shows prediction of subharmonic edge wave model with ε = 3. Uncertainties arising from finite simulation size give error bars (calculated as mean spacing divided by number of cusps).

erosion or deposition at all points on the cusp. In the simulations, cross-shore cusp dimension is equal to the horizontal swash excursion S. Steady-state beach cusp spacing, λ_{so}, is observed to be proportional to S (Fig. 3). This result agrees with field observations and the swash circulation model of Dean and Maurmeyer (6; see also *14*). The slope of the line is a geometrical parameter, f, the ratio of cusp spacing to swash excursion. The value of f varies with the details of the algorithm, including water particle interactions and smoothing, but lies between 1 and 3 for simulated cusps. This ratio is not a free parameter of the model (*15*).

A simple scaling argument can be used to explain why $f = \lambda_{so}/S$ is constant for given flow and sediment transport characteristics. The trajectories of water particles obeying the kinematical equations are independent of scale (λ_{so}) for geometrically similar cusps (constant f). Additionally, the net erosion per unit length of travel by a water particle, $2\alpha g \sin\beta'$, is independent of scale, where $\tan\beta'$ is the beach gradient projected along the water particle trajectory, the sediment carrying capacity ($C = \alpha v^2$) defines α, and v is the water particle velocity (*16*). This scale independence implies that if cusps with a particular spacing (λ_{so}) and shape (f) are stable (zero net erosion), cusps with a different spacing (λ^*_{so}) and the same shape ($f^* = f = \lambda^*_{so}/S^*$) also are stable. Therefore, stable cusps of different sizes can have the same shape, and f is a constant. Viscous or turbulent energy losses and swash percolation into a porous beach can cause a dependence of f on S.

The agreement between predicted and observed cusp spacing has been cited as evidence in favor of the standing wave model (*4*). However, the parameters in the standing wave and self-organization models can be related so that the two models predict a cusp spacing that differs only by a factor close to 1. The subharmonic edge wave model predicts that cusp spacing is $\lambda_{ew} = (\sin\beta/\pi) g T_i^2$; (*3*), where T_i is the incident wave period. The self-organization model predicts that spacing is $\lambda_{so} = fS$. The quantity S increases linearly with offshore wave amplitude but saturates as a result of wave breaking at a value specified by the dimensionless relation $\varepsilon = 2\pi^2 S/(\tan\beta g T_i^2)$ (*17, 18*). At saturation, the parameter ε is between 2 and 3 for laboratory measurements (*17, 19*) and in the range 2 to 12 on a natural beach (*20*). For saturated or near-saturated swash, the ratio $\lambda_{so}/\lambda_{ew} = f\varepsilon/(2\pi\cos\beta)$ is a constant close to 1. Therefore, measurements of cusp spacing cannot be used to discriminate between the two models without more precise measurements of f, ε, and β during cusp formation and a theoretical assessment of the limitation to monochromatic waves on the predictions of the edge wave model, both of which are lacking.

Any model that can explain beach cusp formation should also be able to predict conditions under which beach cusps do not form, particularly because cusps are rare on most beaches. Beach cusps tend to form with normally incident, nonbreaking waves and high beach slopes, all conditions conducive to the development of standing subharmonic edge waves. Computer-simulated cusps develop only at small water particle angles incident on the beach (for example, less than 10° on a beach with a 5° slope) because at higher incident angles, initial channels (incipient bays) formed on runout cross and obliterate mounds of deposition (incipient horns) formed on runup. Cusp formation on beaches with low slopes ($\beta <$ 1.5° for the parameters used in Fig. 2) is suppressed in the simulations because deposition and erosion of sediment in a single swash cycle is spread out over a distance larger than that for steeper beaches. As a result, local depressions that form are too small for significant deflection of water particles and the consequent positive feedback growth of incipient relief. One effect of breaking waves is turbulence in the surf and swash zones that can cause random fluctuations in swash flow. Simulated cusp initiation is hindered by the application of random forces to water particles when the magnitudes and durations of these forces are similar to the gravitational forces that attract swash particles toward incipient relief. Therefore, both standing wave and self-organization models can explain qualitatively the conditions under which beach cusps do not form.

The development of beach cusps is believed to damp the amplitude of subharmonic edge waves. It has been argued that this damping is the mechanism for stabilization of beach cusps (*8*) or that edge waves provide only the initial perturbation for cusps, which thereafter are formed (with a spacing corresponding to the edge wavelength) by feedback between flow and morphology (*4*). To test whether cusps will form by flow-morphology feedback at a spacing determined by edge waves, we created in our model cuspate features in the beach with uniform spacing unrelated to swash excursion (such as could be formed by edge waves) and subjected them to hundreds of swash cycles. Cusps reformed at the spacing predicted by the self-organization model (proportional to swash excursion). The conditions that are necessary for self-organized cusp formation, coupling between alongshore surface gradients and flow, are unfavorable for cusp formation in the standing wave model. Therefore, we conclude that the standing wave and self-organization mechanisms are incompatible.

In the standing wave model, it is assumed that flow and the resulting sediment transport are driven by gradients in sea-surface elevation (morphology) that arise from wave patterns. The self-organization model relies on a coupling between flow and bottom morphology. Remarkably, these two incompatible, physically distinct mechanisms lead to similar predictions for spacing and formation conditions of beach cusps over a wide range of scales. Discrimination between the two mechanisms likely will require detailed observations of morphology and swash flow during cusp formation.

REFERENCES AND NOTES

1. P. D. Komar, *Beach Processes and Sedimentation* (Prentice-Hall, Englewood Cliffs, NJ, 1976).
2. _____, *Geol. Soc. Am. Bull.* **84**, 3593 (1973).
3. R. T. Guza and D. L. Inman, *J. Geophys. Res.* **80**, 2997 (1975).
4. D. L. Inman and R. T. Guza, *Mar. Geol.* **49**, 133 (1982).
5. D. W. Johnson, *Geol. Soc. Am. Bull.* **21**, 599 (1919).
6. R. G. Dean and E. M. Maurmeyer, in *Proceedings of the 17th Coastal Engineering Conference* (American Society of Civil Engineers, New York, 1980), p. 863.
7. R. T. Guza and R. E. Davis, *J. Geophys. Res.* **79**, 1285 (1974).
8. R. T. Guza and A. J. Bowen, *ibid.* **86**, 4125 (1981).
9. A. H. Sallenger, *Mar. Geol.* **29**, 23 (1979).
10. Subharmonic signals have been observed during beach cusp formation (*21*). However, the alongshore pattern of a standing wave was not observed. Subharmonic signals can arise from mechanisms other than standing subharmonic edge waves (*22, 23*).
11. M. C. Shen and R. E. Meyer, *J. Fluid Mech.* **16**, 113 (1963).
12. H. H. Yeh, A. Ghazali, I. Marton, *ibid.* **206**, 563 (1989).
13. For example, R. A. Bagnold, *Proc. R. Soc. London Ser. A* **249**, 235 (1956).
14. M. S. Longuet-Higgins and D. W. Parkin, *Geogr. J.* **128**, 194 (1962).
15. The precise value of f is determined by the details of models for the hydrodynamical interactions in the swash and the diffusive transport of sediment. Future refinements of the swash flow model should allow us to predict a value for f in a more narrow range. The uncertainty in f is commensurate with uncertainties related to a distribution of incident wave frequencies for the edge wave model (*4*).
16. The net erosion by a swash particle between two closely spaced points on the beach labeled 0 and 1 is the change in carrying capacity $\Delta C = \alpha(v_1^2 - v_0^2) = -\alpha 2g\Delta h$, where v_i is the velocity at point i and Δh is the elevation change going from point 0 to point 1. The net erosion per unit length of travel, s, is then independent of cusp scale: $\Delta C/s = -\alpha 2g\Delta h/\Delta x_{01} = -\alpha 2g\sin\beta'$, where Δx_{01} is the distance between points 0 and 1.
17. R. T. Guza and A. J. Bowen, in *Proceedings of the 15th Coastal Engineering Conference* (American Society of Civil Engineers, New York, 1976), p. 560.
18. R. T. Guza, personal communication.
19. W. G. Van Dorn, *J. Geophys. Res.* **83**, 2981 (1978).
20. R. T. Guza and E. B. Thornton, *ibid.* **87**, 483 (1982).
21. D. A. Huntley and A. J. Bowen, in *Proceedings of the 16th Coastal Engineering Conference* (American Society of Civil Engineers, New York, 1978), p. 1378.
22. _____, in *Nearshore Sediment Dynamics and Sedimentation*, J. R. Hails and A. Carr, Eds. (Wiley, New York, 1975), pp. 69–109.

23. G. Wallerstein and S. Elgar, *Science* **256**, 1531 (1992).
24. We thank R. T. Guza for discussions and for reviewing the manuscript. S. A. Herndon rendered Fig. 2, and T. A. Tombrello facilitated our collaboration. The Office of Naval Research, Coastal Sciences [N00014-92-J-1095]; the Mellon Foundation; and the Division of Physics, Mathematics and Astronomy, California Institute of Technology, provided support.

12 November 1992; accepted 10 February 1993

Geography of End-Cretaceous Marine Bivalve Extinctions

David M. Raup and David Jablonski

Analysis of the end-Cretaceous mass extinction, based on 3514 occurrences of 340 genera of marine bivalves (Mollusca), suggests that extinction intensities were uniformly global; no latitudinal gradients or other geographic patterns are detected. Elevated extinction intensities in some tropical areas are entirely a result of the distribution of one extinct group of highly specialized bivalves, the rudists. When rudists are omitted, intensities at those localities are statistically indistinguishable from those of both the rudist-free tropics and extratropical localities.

The Cretaceous-Tertiary (K-T) mass extinction marked the end of the Cretaceous period and the Mesozoic era and caused a 60 to 80% reduction in global biodiversity at the species level (*1*). This extinction is far better documented than any other such event in the geologic past and thus provides the best opportunity to explore environmental or other stresses that can cause mass extinction. Comparison of victims and survivors with regard to their habitats, physiologies, and geographic distributions should aid understanding of the causes and nature of this extinction. Here, we explore geographic patterns in the K-T extinction using a global analysis of marine bivalves (Mollusca). We evaluate whether there were local "hot spots" (*2*) of extinction, whether one hemisphere was affected more or less severely, and whether there were regular latitudinal or other gradients.

The K-T extinction has often been portrayed as more severe in the tropics than in temperate or polar regions (*3*), although paleontologic data on this point have been sparse and taxonomically scattered. Our database contains 3514 occurrences of 340 genera of bivalve mollusks from 106 assemblages of Maastrichtian (uppermost Cretaceous) marine fossils (Fig. 1). We chose bivalves because they were an important component of Cretaceous marine bottom communities, their taxonomy is well known and reasonably stable, and their average extinction rate is well suited for statistical analysis (63% of Maastrichtian bivalve genera did not survive into the Tertiary period). Few other biologic groups have these qualifications. Furthermore, bivalve data have been used extensively to support the inferred latitudinal gradient in K-T extinctions (*3*).

Most of the 106 assemblages were drawn originally from published sources (*4*) but were subjected to an updating and evaluation procedure, including consultations with experts on subgroups or specific geographic areas and examination of museum collections (where possible), in order to minimize taxonomic and stratigraphic inconsistencies. Species in lists from the older literature were shifted according to modern genus definitions, and some local names were eliminated.

We did not attempt to subdivide the Maastrichtian interval in this analysis. Finer stratigraphic resolution would be valuable but is impossible on a global basis because of uncertainties in dating and correlation: a sample confined to assemblages of proven latest Maastrichtian age would be too small for meaningful geographic analysis. Thus, our results apply to extinction at the K-T boundary event only to the extent that Maastrichtian extinctions were concentrated at that event. Although dilution by extinction within the Maastrichtian is probably minor, the interval does encompass considerable environmental fluctuation (*5*), and some extinctions, such as that of inoceramids and rudists, may have preceded the K-T event and thus would blur our results.

The choice of an extinction metric for the analysis is critical. Ideally, Cretaceous assemblages should be compared with those in the immediately younger Tertiary deposits of the same area. However, there are so few truly continuous sequences across the K-T boundary, with comparable habitats and fossil preservation, that the usable sample is far too small to be robust. Therefore, extinction was quantified as the proportion of genera found in an assemblage, or local group of assemblages, that suffered global extinction in the final stage of the Cretaceous. This metric has the advantage of making use of the excellent compilations of global extinctions for the K-T boundary (*6*), but it has the disadvantage that genera may die out in one area, perhaps a hot spot, yet survive globally because they also lived outside the area. These genera would be labeled survivors; thus, the actual species kill in the local area would be underestimated. However, endemism in our database is sufficiently pronounced (22% in North

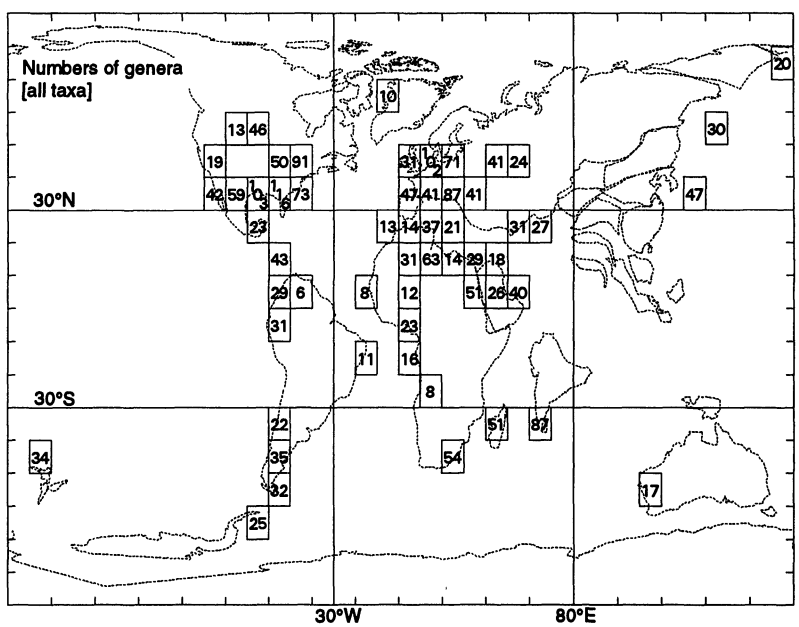

Fig. 1. Sample sizes in the 57 10° latitude-longitude blocks that contain one or more of the 106 bivalve assemblages (*20*), plotted on Maastrichtian geography. Rudists are included.

Department of the Geophysical Sciences, University of Chicago, 5734 Ellis Avenue, Chicago, IL 60637.